



UNITED NATIONS  
UNIVERSITY

**UNU-GTP**

Geothermal Training Programme

Orkustofnun, Grensasvegur 9,  
IS-108 Reykjavik, Iceland

Reports 2014  
Number 24

## **APPLICATION OF STABLE ISOTOPE GEOCHEMISTRY TO TRACING RECHARGE AND FLOW SYSTEMS OF FLUIDS IN THE OLKARIA GEOTHERMAL FIELD, KENYA**

**Melissa Nailantei Nkapiani**

Kenya Electricity Generating Company – KenGen

P.O. Box 785 – 20117, Naivasha

KENYA

*mnapiani@kengen.co.ke*

### **ABSTRACT**

The long term success of any geothermal energy utilization depends on understanding groundwater movements and recharge areas. Water and steam condensates from subfields in the Olkaria geothermal field have been studied using the stable isotope ratios of hydrogen and oxygen to gain information on thermal fluid flow and to trace the origin of thermal waters.

Isotope fractionation factors and mass balance equations were used to characterize reservoir fluid composition of wells in the area, assuming single stage steam separation. Comparison of the two methods yields coherent results for the oxygen-18 isotope ratio, but the deuterium isotope ratio varies to some extent. The reservoir fluid isotope composition of the thermal waters suggests three recharge zones for the field: one from groundwater from the eastern Rift wall with  $\delta D$  about = -24‰; groundwater from the western Rift flank with  $\delta D$  about = -30‰; and the other from an evapo-concentrated source with  $\delta D$  about = 36‰. Qualitative interpretation of the available data suggests that the evapo-concentrated source largely contributes to the recharge of the East field, North East field and a part of the Domes field. Groundwater from the western rift wall recharges the West field of the area. The eastern Rift wall groundwater contributes to the southeast part of the Domes field.

The isotopic composition of some thermal waters in the Olkaria geothermal field indicates that there could be groundwater mixing between the waters from the flanks and the evapo-concentrated source. The chloride content of the recharge water cannot be used to determine the degree of mixing between these recharge zones because of the similar content of chloride in both types of water. Evolution of the water isotope composition of the well fluids over time indicates possible temporal variations related to the recharge zones. More data from boreholes and springs in the area must be collected to monitor the variations and evolution of water isotope composition in the field.

### **1. INTRODUCTION**

The Olkaria geothermal field is a high temperature geothermal field located in the Kenya Rift valley about 120 km from Nairobi. The Kenya Rift valley is part of the East Africa Rift System (EARS) which

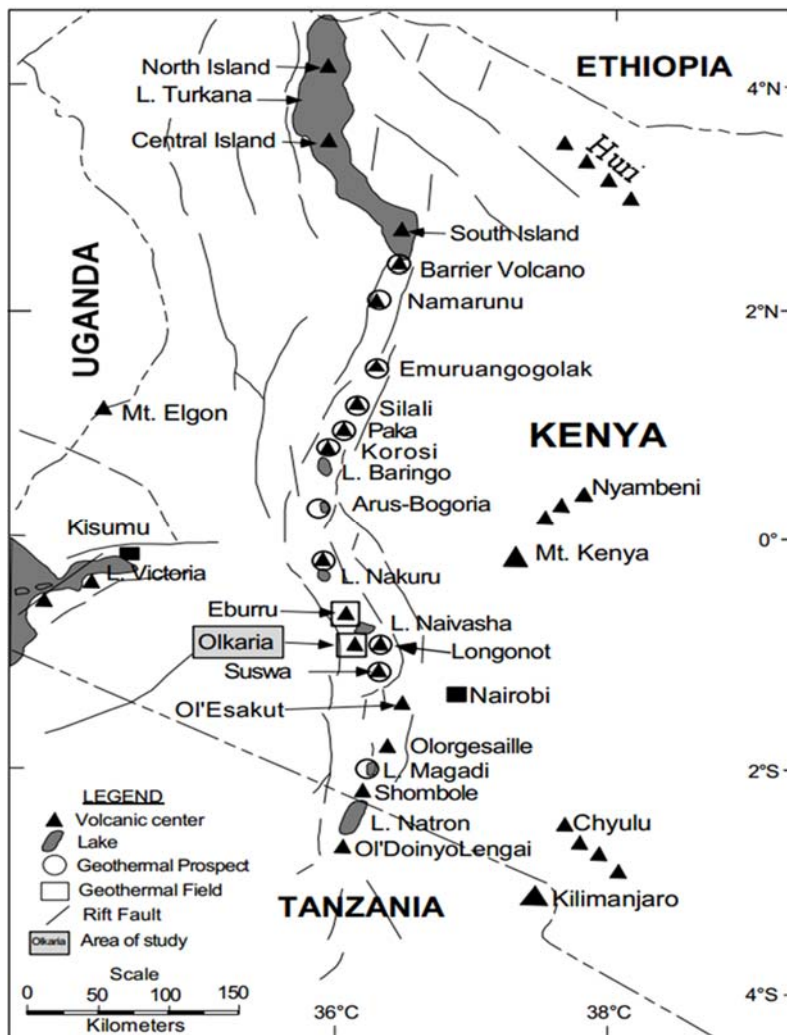


FIGURE 1: A map of the Kenya Rift Valley System showing the location of the Olkaria geothermal field

runs from the Afar triple junction at the Gulf of Aden in the north to Mozambique in the south. In Eastern Africa, the Rift system splits into two: the Western Rift valley and the Eastern Rift valley with the Kenya Rift being a segment of the Eastern Rift valley. Figure 1 shows the location of the Olkaria geothermal field in the Kenya Rift System. The geothermal system at Olkaria has been used to generate power since 1981. The area is divided into 4 subfields for purposes of development and utilization. These include: Olkaria East (Olkaria I), Olkaria Northeast (Olkaria II) Olkaria West (Olkaria III) and Olkaria Domes (Olkaria IV). The Olkaria East field currently generates 45 MWe. An additional plant is under construction in the same field and is expected to host a 140 MWe power station. The Olkaria Northeast field hosts a power station generating 105 MWe. The Olkaria West field, which has been developed by IPP-Orpower Inc., generates 105 MWe using binary technology. The Olkaria IV power plant, located in Olkaria Domes, has recently been

commissioned and 2 single flash condensing turbines are used to generate 140 MWe. This brings the total installed electric capacity for the Greater Olkaria Geothermal area up to around 400 MWe. All these plants tap steam from wells drilled down to about 3000 m depth. Drilling and well discharge testing is still ongoing in all these fields to provide steam for new plants.

Subsurface drainage from Lake Naivasha, a fresh water lake that lies in the northern part of the Olkaria geothermal field, has led to considerable speculation on the contribution of the lake to the hydrological regime of the area, and the possibility that the subsurface drainage from the lake could actually be recharging wells in the geothermal field. This has provoked an extensive study of the lake catchment area. Hydrochemistry has been treated in the past as an effective way of defining groundwater sources and assessing mixing patterns. In this report, the isotope characteristics of waters in the Olkaria geothermal fields are reviewed and a conceptual hydrological model of the area is postulated.

### 1.1 Geological setting of the Olkaria volcanic complex

The Rift valley system is characterized by numerous volcanic centres of Quaternary age. The Olkaria volcanic complex is one of them. Adjacent to the volcanic complex is the Longonot volcano to the southeast and Suswa to the south, shown in Figure 1. Eruptions associated with the Olkaria volcano and

the Ololbutot fault zone have produced rhyolitic and obsidian flows, while eruptions in the Longonot and Suswa volcanoes have ejected pyroclastic ash which has blanketed much of the area (Lagat, 2004). Acidic lavas and their pyroclastic equivalent characterize the surface and near subsurface geology of the Olkaria geothermal field, which is inside a major volcanic complex that has been intersected by N-S trending normal faults. The main features of the structural geology of the volcanic complex, shown in Figure 2, include the ring structure which is characterized by numerous volcanic domes, interpreted as indicating the presence of a buried volcanic caldera. From the correlation of stratigraphy and alteration mineralogy zones in Olkaria, it can be deduced that the most prominent features are normal faults. The oldest faults follow the regional NW-SE trend and they define the shape of the stretched buried caldera: the

Gorge farm fault, Olkaria fracture and Suswa fault. Other younger faults include an ENE-WSW Olkaria fault and the Ololbutot fault, the Olkaria fracture and the OI Njorowa Gorge trending in an N-S direction. The subsurface geology is characterized by tuffs, rhyolites, basalts and trachytes with minor intrusives. Structural features, including faults, dykes and intrusions, control the types and nature of fluid-rock interaction processes as well as fluid movement within the geothermal system (Mwania et al., 2014).

The first appearance of epidote (above 240°C) marks the upper limit to the Olkaria geothermal reservoir. The epidote zone is associated with the occurrence of high temperature clays like illite and chlorite. The zone occurs at a depth of about 500 m b.g.l. in the up-flow zones, and at around 800 m b.g.l. in the out-flow zones and sometimes deeper in the down-flow zones. Four (4) hydrothermal alteration assemblages defined by the first appearances of specific index minerals occur in the field including: a smectite-chlorite-illite zone (<300 m b.g.l.); a chlorite-illite zone (300-550 m b.g.l.); an epidote-chlorite-illite zone (550-1400 m b.g.l.); and an actinolite-epidote-chlorite-illite zone (1400-3000 m b.g.l.). The shallower occurrence of the high temperature mineral assemblages marks the upflow zone in the field. Three (3) major upflow zones, determined from the updoming of the alteration mineralogy and current measured temperatures in the Olkaria fields, were observed in the East/Northeast, Domes and Southeast fields (Mwania et al., 2014).

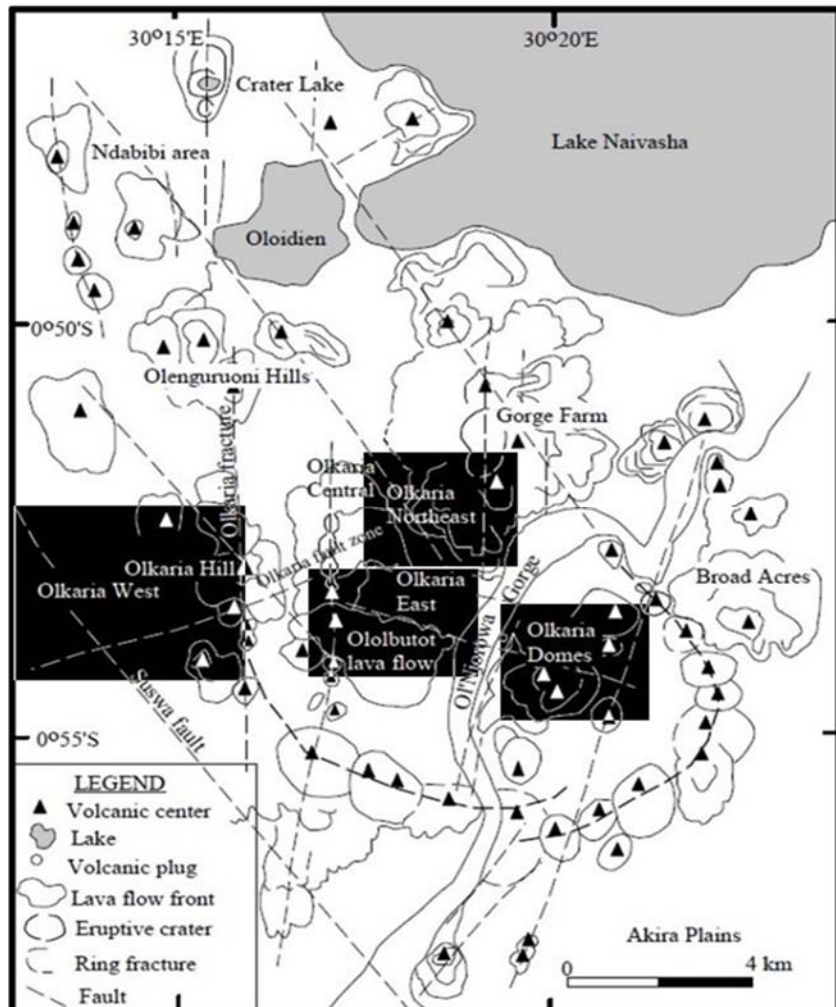


FIGURE 2: Structural geological map of the Olkaria geothermal field, from Clarke et al. (1990) also showing the study areas

## 2. HYDROGEOLOGY OF THE RIFT VALLEY SYSTEM

The long term success of any geothermal energy utilization depends upon the understanding of groundwater movements and recharge areas. The hydrogeology of the Rift valley system has been extensively studied and reported by several authors. Allen et al. (1989), in their phase I report, collected physical hydrogeological data from over 600 boreholes drilled between the Tanzanian border in the south to Nakuru in the north. From the analysis of the data, they show that on a regional scale the Rift Valley system between Lakes Magadi and Lake Nakuru broadly exhibits the hydrogeological features observed for a valley - interfluvial system with prominent lateral groundwater flows from the Rift escarpment to the discharge areas on the Rift floor. In their phase II report, Allen and Darling (1992) studied the physical hydrogeology of the section of the Rift valley between Lake Baringo in the south and Lake Turkana in the north and also covered several quaternary volcanoes in the centre of the Rift, in particular Korosi, Paka, Silali and Emuruangogolak. From these, they obtained rainfall data from over 38 meteorological stations, surface water data and data from 70 boreholes, comparably lower than the number of boreholes used in the hydrogeological study of the area between Lake Magadi and Lake Nakuru. This is because this section of the Rift system is an arid and sparsely populated area where evaporation is evident and, therefore, called for the need to use indirect methods to assess groundwater conditions. Figure 3 shows a piezometric map designed by Allen and Darling (1992), based on lithological information, hydraulic data and construction details from boreholes drilled on Rift walls as well as from the Rift floor. The data they collected was used to construct a piezometric map of the southern part of the Kenya Rift. From this work they concluded that areas of groundwater recharge are on the east and west flanks of the Rift walls and discharge areas are on the Rift floor. Therefore, both Allen et al. (1989) and Allen and Darling (1992) concluded that the Rift floor obtains its groundwater recharge from the Rift escarpments, where substantial rainfall is present through grid faulting acting as channels for underground water; it has been suggested that these grid faults are quite active, implying that they are open.

Hydrogeologically, the structure of the Rift valley and, in particular, the major Rift faults and the system of grid faulting on the Rift floor, has a substantial effect on the groundwater flow systems of the area. Faults may facilitate flow by providing channels of fluid flow or they may be barriers to flow. Faulting in the Rift system along the axis of the Rift is mainly grid faulting. That is to say fluids flow along the axis of the Rift system and, therefore, cause groundwater flows from the flanks of the Rift towards the Rift floor to follow longer paths, reaching greater depths, and to align flows within the Rift along its axis. Therefore, groundwater flows from elevated recharge areas to low lying discharge areas, in this case to the Rift floor, where the Olkaria geothermal field is located.

### 2.1 Hydrogeology of Olkaria geothermal field and Lake Naivasha catchment

The Rift area around the Olkaria geothermal field is bounded by the Mau escarpment in the west, rising to an altitude of up to 3000 m, and the Nyandarua – Kikuyu Escarpment in the east, with an elevation of 3999 m. The area is further bounded by a relatively high lying fault, particularly the Kinangop plateau of 2100 m elevation in the Eastern rift. The floor of the Rift valley culminates near Lake Naivasha at 1884 m. Rivers Malewa and Gilgil, being perennial rivers, provide much of the recharge to the lake besides local precipitation. The Gilgil River has its headwaters high in the Bahati forests and drains parts of the eastern slopes of the Bahati escarpment. River Malewa is believed to derive its recharge from the western slopes of the high Nyandarua range (Allen et al., 1989). The lake has no surface outlet but still remains a fresh water lake in an area where evaporation rates are very high. This, therefore, indicates that this lake, which is located in the southern part of the Rift floor, has some subsurface drainage. Several researchers have tried to quantify subsurface discharge from the Lake Naivasha catchment area. McCann (1972) carried out a comprehensive hydrogeological study of the Rift valley catchment area and was able to quantify the groundwater flows of Lake Naivasha by defining evaporation rates, and the water inflow from direct precipitation and evapotranspiration values and, thus, arrived at a value of  $34 \times 10^6 \text{ m}^3/\text{yr}$  as groundwater outflow from the lake. McCann (1974) and Sikes (1935) also used water

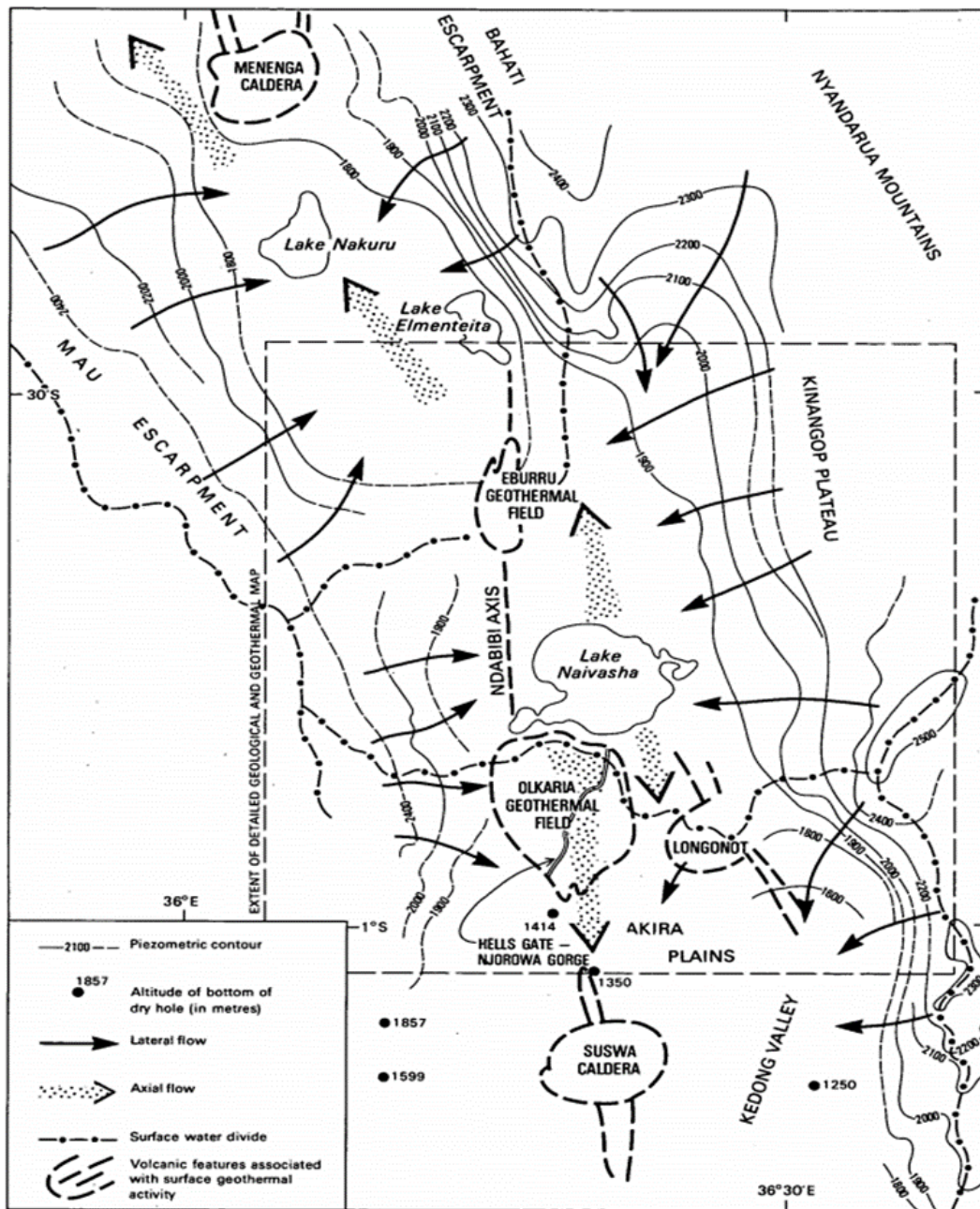


FIGURE 3: A piezometric map of the Kenya Rift Valley System, adapted from Allen et al. (1989)

balance studies, and estimated subsurface discharge from the lake as  $43 \times 10^6 \text{ m}^3/\text{yr}$ , which agrees reasonably well with McCann's values of  $34 \times 10^6 \text{ m}^3/\text{yr}$ . Panichi and Tongiorgi (1974) used an isotopic model and defined the isotope signatures of the influent waters and the lake water, as well as the evaporation from the lake, and arrived at a value of  $254 \times 10^6 \text{ m}^3/\text{yr}$  as the groundwater recharge, much higher than the values reported by Sikes (1935) and McCann (1972). Allen et al. (1989) did stable isotope studies, recalculated the values obtained by Panichi and Tongiorgi (1974), and arrived at a value of  $52 \times 10^6 \text{ m}^3/\text{yr}$  as the groundwater drainage from Lake Naivasha, close to what previous researchers obtained. So the subsurface drainage from Lake Naivasha can be estimated to be  $50 \times 10^6 \text{ m}^3/\text{yr}$ . The Naivasha catchment area is a more hydrogeologically complex environment, receiving water from direct precipitation and from the Rift flanks, either as stream flows or a subsurface flow, and discharging to the southern and northern sides as stated by various authors, particularly, McCann (1972) who used piezometric levels to suggest that the water from the lake was flowing in both northerly and southerly directions. Allen et al. (1989) used regional head gradients and permeability to try to quantify the

northern and southern flows and, according to their results, a north - south groundwater gradient of 0.05m/m exists over the Olkaria –Longonot area, and 0.1m/m in the Olkaria field, taking into account the estimated hydraulic conductivity of the area, and taking 5 km as flow depth. The southern flow at depth from Lake Naivasha was estimated to be  $41 \times 10^6 \text{ m}^3/\text{yr}$ .

The Olkaria geothermal field is located south of the lake; therefore, the recharge to this field could possibly be connected to groundwater on the Rift floor. Allen et al. (1989) used stable isotopes to trace Lake Naivasha's water. They found out that river waters discharging to the lake have a very depleted isotope composition, indicative of their origin at higher altitudes, more specifically the Nyandarua ranges. This is facilitated by major Rift faults, which act as conduits for lateral flow or barriers which lead to deeper flow paths, and by grid faulting, which tends to align flow paths within the Rift along its axis. However, the lake water is enriched in stable isotope ratios due to evaporation to which it is subject. They also indicated that the lake water appeared to be detected at least 30 km to the south of Suswa volcano, which is to the south of the Olkaria geothermal field. Arusei (1991) used halide ratios, a Cl/Br ratio diagram, to determine whether Lake Naivasha has an exposed groundwater table and also to determine the origin of recharge to wells in the Olkaria geothermal fields. He concluded that there exists a correlation between the escarpment Rift floor and geothermal waters and showed that the Olkaria geothermal reservoir gets recharge water from either the Rift groundwater or the escarpment waters, although he was not able to infer a single recharge from any of this. He was also able to conclude that Lake Naivasha is not an exposed groundwater table, since the concentrations of many of the constituents increase away from the lake. For this reason, he concluded that the flow in the lake is both in northern and southern directions.

Much cannot be done regarding hydrology if subsurface structures are not mentioned, because fractures control fluid movement to a great extent. The movement of water from the escarpment to the Rift floor is complicated by the geological structures present in this area. Understanding subsurface structures and hydrothermal alteration of the Olkaria geothermal area is essential in determining the characteristics of the reservoir and the behaviour of the geothermal fluid. The existence of faults and other structural features, like dykes and intrusions, is paramount in geothermal utilization, because they control the types and nature of the water rock interaction processes, as well as the fluid movement within the system. It is also necessary to determine the influence of the faults in the existing fault pattern and to map the fluid flow through available channels. Fault systems in the field include ENE-WSW, NW-SE, N-S, E-W structures and are associated with fluid movement. They are all defined as normal faults through the correlation of lithology and alteration mineralogy zones. These faults include the N-S faults (Ololbutot fault, Olkaria fracture and Olnjorowa Gorge), ENE-WSW (Olkaria fault) NW-SE (Gorge farm fault) and the Ring structure. These faults control fluid movements and also impact mixing fluid patterns.

### **3. FLUID CHEMISTRY**

#### **3.1 Characterization of fluid chemistry in Olkaria geothermal field**

The East field is characterized by a shallow steam-dominated zone of >300 m thickness overlying a liquid reservoir. A deep liquid reservoir is present in the Domes field, which is evidenced by the chemistry of the fluids discharged, as well as from the temperature and pressure profiles reported for this field. Discharge data and production field monitoring data show a fairly high enthalpy in the Olkaria East and Northeast fields, with reported enthalpy values of >2100 kJ/kg. The West field enthalpy data show a fairly low enthalpy compared to the rest of the fields. In the Domes field, saturated liquid enthalpy is observed in the northwest part of the area, but high enthalpy in the southeast part. Various water types are discharged from these fields, evident from the reported chemistry of the fluids. Table 1 shows the chemical composition of well fluids used for isotope studies. The Olkaria East field discharges mostly fluids of the Na-Cl type with slightly elevated sulphate levels. This could be interpreted as showing the presence of an upflow zone. The Olkaria Northeast field also discharges fluids with Cl in

TABLE 1: Chemical composition of wells in Olkaria geothermal field

Well	Year	WHP (bar-g)	GSP (bar-g)	Enthalpy (kJ/kg)	pH@ 20°C	SiO <sub>2</sub>	B	Na	K	Ca	Mg	CO <sub>2</sub>	SO <sub>4</sub>	H <sub>2</sub> S	Cl	F	CO <sub>2</sub>	H <sub>2</sub> S	H <sub>2</sub>	CH <sub>4</sub>	N <sub>2</sub>
2	1988	4.5	4.2	2287	9	741	4.4	1067	190	0.7	0.1	126.7	47	0.14	813.5	0.072	110.7	3.64	6.94	1.07	2.91
4	1987	1.4	5.5	1533	8.7	635	2.9	362	65	0.3	0.1	88	15	0.9	500	68	104	6.42	4.07	0.28	4.52
6	1988	5	4.6	2378	8.88	541	8	398	51	2.68	0.14	76	24	0.23	759	45	160.1	2.28	9.18	1.46	0.66
10	1988	5.4	4.1	2457	8.48	482	13	769	106	0.24	0.13	62.5	99	0.9	882	123	131.1	7.53	9.5	0.72	0.11
11	1988	5.5	4.5	2222	8.85	601	7	479	75	0.88	0.5	102	40	0.27	677	83	105.8	1.95	6.23	0.77	0.15
13	1988	5	4.6	2400	9.65	857	4.2	415	59	1.39	0.2	251	24	4.45	351	83	96.7	1.81	13.31	0.46	1.43
14	1984	5.6	4.4	2600	5.75	638	1.52	584.5	102.3	0.6	0.39	116.1	89	0.34	582.4	52.85	174.8	5.8	15.55	0.33	0.68
15	1988	5	5	2600	8.8	447	4.1	920	151	2.19	0	133	100	17	1369	88	105.8	2.57	9.55	0.51	0.67
16	1988	5	4.8	2150	8.79	696	4.6	475	63	0.47	0	108.2	17.7	0.48	621	84	122.7	2.89	7.77	0.54	0.54
17	1987	4.8	4.2	2600	9.7	724	6.2	1092	168	3.7	0.08	246	77	1	1308	60	55.7	12.21	13.29	0.56	9.02
18	1988	7.5	4.5	2596	8.66	557	4.9	845	132	0.91	0.12	151	57	0.17	1273	125	81.6	2.45	0.43	0.29	10.69
19	1987	5	4.5	2500	9.15	689	10.3	666	124	0.7	0.03	57.2	61	2.7	796.2	104	275.3	25.2	10.62	0.73	0.49
20	1988	5	5	2300	8.85	676	8.1	566	90	1.24	0	141	43	0.54	894	95	78.1	2.44	8	0.17	0.42
21	1988	5	4.5	2390	9.5	643	4.6	436	72	0.96	0.08	290	137	6.39	401	63	168.1	3.65	11.69	0.37	1.95
22	1988	6	5	2610	9.63	488	3	492	70	1.22	0	290	34	6.8	298	61	198.7	3.65	10.85	0.27	0.82
23	1988	6	4.6	2400	9.44	643	4	350	43	0.99	0.15	226	20	1.6	259	161	81.5	3.16	10.13	0.16	0.77
24	1987	5	4.5	2460	9.09	732	8	659	126	0.7	0.4	114	78	0.2	800	124	143	4.65	10.01	0.59	0.67
25	1988	5	5	1920	9.03	726	4.2	583	130	0.65	0.5	141	32	1.2	658	69	81	183.8	3.26	8.62	0.27
26	1988	5.5	4.6	2025	9.37	599	3	408	70	0.1	0.06	102.1	38	1.6	282	52	223.3	11.86	12.99	0.39	0.62
701	1987	4.1	3.1	1255	9.4	605	3.4	476	92	0.81	0.05	128	90	4.76	685	50	228	8.79	6.14	0.73	2.7
703	1989	5.4	5.3	1820	9.5	509	3	719	144	0.43	0.06	180.4	37	0.61	946	81	129.3	1.86	5.08	0.68	1.04
709	1993	1.2	0.7	1047	10.17	682	4.7	290	102	0.3	0	191.1	71	2.72	703	48	122.2	0.62	0.01	0.09	2.45
714	1991	19.3	2.8	1125	9.64	649	5.5	594	123	0	0	211	42	10.2	684	57	174.1	9.9	2.42	0.54	4.31
719	1998	3.1	2.1	1038	9.3	700	5.6	690	90	0.2	0	345.3	26.2	23.18	604	83	498.4	22.68	5.7	1.06	11.32
301	2000	7.4	1.5	1180	8.67	855	6.8	1283	208	0.66	0.07	578	112	3.96	240	105	426.1	3.55	11.27	0.83	1.05
302	2000	5.7	1.8	1130	9.72	744	3.5	633	101	1.04	0.08	578	54	3.43	505	77	367.5	1.11	3.22	0.38	0.33
304	1999	3.9	2.6	875	8.13	364	3.3	959	74	3.48	1.73	1752	93	0.97	52	24	11462	2.66	7.37	1.72	0.94
306	1999	4	1.8	1019	9.15	551	6.3	850	96	1.2	0.08	1081	50	2.9	251	62	1136.8	2.89	7.83	0.94	0.56
901	1999	6.2	0.7	1600	9.36	636	5.7	453	73	0	0	361.6	47	16.5	290	77.7	339	23.7	10	1.5	6
902	1999	3.3	1	1338	9.61	800	2.6	509	37	0	0	482.8	109	2	205	52.3	361	1.9	18.94	1.8	0.63
903	1999	3.8	1.4	1073	9.8	611	1.66	571	39	0	0	706	108	1.1	178	46.6	341	0.9	18.94	1.8	0.63
914A	2010	2	3.2	2236	9.81	613.5	2.68	953.7	163.1	1.24	0	820.16	52.4	1.83	306	887.7	0.53	14.87	2.21	2.21	21.31
916A	2010	6	4	2500	9.46	570	3.46	525.1	184.2	1.32	0.56	301.18	67.9	1.63	323.4	235.2	225.9	0.43	14.87	1.22	21.31

excess of  $\text{HCO}_3$ , except for a few wells. The West field water is predominantly of the bicarbonate type, which could be indicative of peripheral waters. In the Domes field, a mixture of fluids is produced, both Na-Cl and  $\text{HCO}_3$  waters. It is clear from the water types discharged in these fields that subsurface geological structures control the movement of recharge fluids, as well as the fluid types observed in these areas.

Applications of the Na/K solute geothermometer, proposed by Fournier and Potter (1982), indicate temperatures between  $250^\circ\text{C}$  and  $275^\circ\text{C}$  for the East and Northeast fields, temperatures from  $230$  to  $250^\circ\text{C}$  for the West field, whereas the Domes field waters show temperatures  $>270^\circ\text{C}$ . The Cl distribution in the area delineates upflow zones and, from the interpretation of these chloride distribution maps, four distinct upflow zones are postulated in the East, Northeast, West and the Domes fields.

### 3.2 Application of stable isotope geochemistry

Water is by far the most abundant component of the geothermal fluid and also the major energy carrier in geothermal systems. The application of stable isotope geochemistry mainly involves natural isotopes that form water molecules being used to identify the source and track the movement of water, both on the surface and through underground channels. Table 2 shows the state and abundance of natural isotopes in water molecules. Isotope measurements have been used extensively in geothermal studies to provide information on the characteristics of the geothermal fields, particularly to provide information on mixing between water masses of different origins and temperature, define underground flow patterns and the degree of interaction with the reservoir rock, and also to provide information on the origin of various fluid components. Stable isotopes have proven to be ideal tracers because they are integral constituents of the water molecules.

TABLE 2: The water isotopes

Isotope	Average natural abundance	Half life
$^1\text{H}$	99.985	Stable
$^2\text{H}$	0.015	Stable
$^3\text{H}$	$10^{-15}$	12.43 years
$^{16}\text{O}$	99.76	Stable
$^{18}\text{O}$	0.20	Stable

Subsurface processes change the original isotopic characteristics of geothermal water. The exchange at high temperature, due to water-rock interactions, leads to an increase in the oxygen-18 content of the water, and a subsequent oxygen decrease in the country rock. This phenomenon can be identified on  $\delta\text{D}-\delta^{18}\text{O}$  plots as the  $\text{O}^{18}$  of the water will plot towards less negative values (a positive oxygen shift). A negative oxygen isotope shift may also occur if the  $\text{CO}_2$  content of the fluid is relatively high (Truesdell and Hulston, 1980). Generally, little or no corresponding shift is observed in the deuterium value because rocks contain relatively little hydrogen. Thus deuterium isotope ratio has been used as an excellent tracer in hydrological systems. In this report, the stable isotopes of deuterium and oxygen-18 are used to assess the source of recharge water in the Olkaria geothermal field, and to elucidate possible mixing patterns, and then to conceptualize a recharge model for the system.

According to Giggenbach and Stewart (1982), reservoir waters originating at temperatures above surface boiling, mostly cool as they ascend to the surface. This may be due to conduction, mixing with low temperature fluids or adiabatic boiling as a result of depressurization. Cooling by conduction will not alter the isotope composition of the reservoir fluid, but dilution and boiling have been known to cause characteristic changes to reservoir fluids. In high temperature geothermal systems, fluids boil during their rise to the surface as a result of depressurization, if the pressure is hydrostatic which is common for liquid-dominated reservoirs. Then the corresponding boiling temperatures follow a boiling point - depth curve. These secondary processes, affecting the isotope composition of geothermal fluids during



their rise to the surface, have to be corrected for when making appropriate interpretations of the isotope data. Steam separation due to adiabatic boiling has different effects, depending on the mode of phase separation. Truesdell et al. (1977) suggest two possible processes: a) one stage separation during which steam separates from the liquid continuously but stays with the ascending water, maintaining isotopic equilibrium, and then separates at one temperature, say at the wellhead temperature; and b) continuous steam separation where the steam separates from the parent water continuously as soon as it is formed. They later suggested that an intermediate process between these two processes exists in natural systems, with single step steam separation generally predominating. Generally, the fractionation of deuterium and oxygen-18, as a result of adiabatic boiling, leads to the enrichment of heavier isotopes in the water phase, and their depletion in the vapour phase, although deuterium is known to have a cross-over point at about 220°C, above which the normal fractionation is reversed and the heavy deuterium isotopes concentrate in the vapour phase as opposed to the liquid phase (Bottinga and Craig, 1968). The high rate at which isotopic equilibrium is attained in geothermal systems, between the liquid and vapour phases, defines the isotope distribution between the liquid phase and the vapour phase, assuming that equilibrium has been attained. This, therefore, implies that the distribution between the water phase and the vapour phase is governed by isotopic fractionation factors which are temperature dependent. These factors, denoted as  $\alpha_D$  and  $\alpha^{18O}$ , were defined by Bottinga and Craig (1968) and are expressed in Equations 1 and 2. The relationship between the fractionation factors and the temperature is used later in this report to calculate reservoir fluid composition.

$$\alpha_{\text{effO}^{18}} = \frac{([\text{H}_2\text{O}^{18}]/\text{H}_2\text{O}^{16}) \text{ water}}{([\text{H}_2\text{O}^{18}]/\text{H}_2\text{O}^{16}) \text{ vapour}} \quad (1)$$

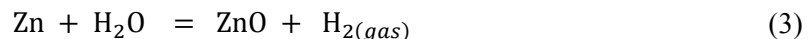
$$\alpha_{\text{eff(D)}} = \frac{([\text{HDO}]/\text{H}_2\text{O}) \text{ water}}{([\text{HDO}]/\text{H}_2\text{O}) \text{ vapour}} \quad (2)$$

Isotope data obtained from fumaroles, springs and lakes are interpreted with respect to the analytical results obtained. This is not the case for geothermal samples obtained from high temperature wells, for example from the Olkaria field. Isotope signatures of samples collected at the surface need to be recalculated to reservoir conditions in order to account for isotopic changes due to boiling and steam loss associated with the mode of phase separation.

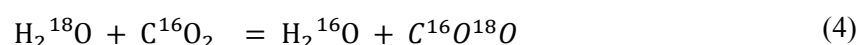
### 3.2.1 Stable isotope analysis and mass spectrometer calculation

#### *Stable isotope analysis*

At the Science Institute, University of Iceland, the stable isotope ratios of oxygen and hydrogen of water were analysed using a Finnigan MAT 251 Mass Spectrometer (prior to 2006) and a Thermo Delta Plus Mass Spectrometer thereafter. The deuterium content in the dataset from Sveinbjörnsdóttir (1988) was determined after reduction to molecular hydrogen (Coleman et al., 1982). Equation 3 shows the reaction involved in the analysis:



In the dataset from Karingithi (2000), the deuterium isotope ratio was determined by the method of Horita (1988), in which the water sample is equilibrated with  $\text{H}_2$  gas using a Pt catalyst. The oxygen-18 ratio was determined after exchange with and determination on  $\text{CO}_2$ , as shown in Equation 4 (Epstein and Mayeda, 1953).



In the datasets from ISOR in 2010 and 2012 (Sekento, 2012), the samples were measured on a Thermo Delta Plus Mass Spectrometer with continuous He flow, using the Gasbench device.

#### *Mass spectrometer calculation*

Absolute concentrations are difficult to determine; therefore, isotope analyses are always presented as relative abundances and, consequently, reported as ratios of proportion of light to heavy species in the

sample relative to those in the standard, for this case VSMOW (Vienna Standard Mean Ocean Water) (Geyh, 2000). Equations 5 and 6 show the methods of computation:

$$\delta_D\text{‰} = \left( \frac{(D/H)_{\text{Sample}} - (D/H)_{\text{VSMOW}}}{(D/H)_{\text{VSMOW}}} \right) 1000 \quad (5)$$

$$\delta_{O^{18}}\text{‰} = \left( \frac{(^{18}O/^{16}O)_{\text{Sample}} - (^{18}O/^{16}O)_{\text{VSMOW}}}{(^{18}O/^{16}O)_{\text{VSMOW}}} \right) 1000 \quad (6)$$

where D/H and  $^{18}O/^{16}O$  represent isotope ratios in the sample and the standard.

### 3.2.2 Isotope composition of fluids

This report entails the interpretation of isotopic data from various subfields of the Olkaria geothermal field during utilization. Hence, several data sets, collected at different times, were used. Table 3 shows the isotopic composition of well fluids while in Table 4 there is mainly data from springs. Sveinbjörnsdóttir (1988) determined isotope ratios in liquid phase and steam condensate samples collected from 19 wells in the East field at 6 bar-a, and from wells OW-701 and OW-703 in the Northeast field. Data for two fumaroles and springs from the Hell's Gate area were also obtained from Sveinbjörnsdóttir's (1988) results. Karingithi (2000) collected liquid phase samples only from the Northeast, West and Domes fields. Results for the boreholes north of Lake Naivasha: Olsuswa and the Ndabibi borehole, were obtained from Sekento (2012). The isotope composition of groundwater from the Rift wall waters was obtained from Allen and Darling (1992). Ojiambo and Lyons (1993) reported isotope ratios for local and Kinangop precipitation.

Isotope analysis reported by Sveinbjörnsdóttir (1988), Karingithi (2000), and Sekento

TABLE 3: Isotope composition of wells fluid in the Olkaria geothermal field

Well	Location	Liquid phase		Steam phase	
		Oxygen ( $\delta^{18}O\text{‰}$ )	Hydrogen ( $\delta D\text{‰}$ )	Oxygen ( $\delta^{18}O\text{‰}$ )	Hydrogen ( $\delta D\text{‰}$ )
<sup>1</sup> 2	East	3.78	18	-0.45	1.3
<sup>1</sup> 4		5.35	32.6	-1.37	-4.2
<sup>1</sup> 16		4.02	17.4	-0.78	-1.5
<sup>1</sup> 10		5.04	27.8	-0.39	1.1
<sup>1</sup> 11		3.78	18.2	-0.39	2.3
<sup>1</sup> 13		4.47	25.3	-0.11	7.5
<sup>1</sup> 14		4.75	25	0.54	9.4
<sup>1</sup> 15		5.51	23.6	0.27	2.6
<sup>1</sup> 16		4.16	17.6	-0.25	-0.8
<sup>1</sup> 17		6.36	32	0.2	4.7
<sup>1</sup> 18		5.46	25.5	0.44	5.6
<sup>1</sup> 19		5.86	29	-0.18	-0.4
<sup>1</sup> 20		4.36	20.2	-0.5	-0.3
<sup>1</sup> 21		6.29	36.3	-0.36	5.1
<sup>1</sup> 22		4.85	26.7	-0.76	2.4
<sup>1</sup> 23		5.7	26	0.49	6.6
<sup>1</sup> 24		4.19	20.3	-0.3	3.2
<sup>1</sup> 25		3.76	17.8	-0.6	-0.5
<sup>1</sup> 26		4.38	24.2	-0.16	6.8
<sup>1</sup> 701	Northeast	3.45	24	-1.06	3.9
<sup>1</sup> 703		4.3	32.9	-1.03	3.7
<sup>2</sup> 709		4.18	23.7		
<sup>2</sup> 714		3.71	23.7		
<sup>2</sup> 719		3.43	22.3		
<sup>2</sup> 301		-0.16	-1.7		
<sup>2</sup> 302		0.87	7.6		
<sup>2</sup> 304		-2.21	-9.3		
<sup>2</sup> 306		-0.04	0.5		
<sup>2</sup> 307		-2.02	-5.8		
<sup>2</sup> 308	-4.55	2.5			
<sup>2</sup> 901	Domes	4.97	32.2		
<sup>2</sup> 902		3.22	21.8		
<sup>2</sup> 903		3.09	21.7		

<sup>1</sup> (Sveinbjörnsdóttir, 1988), <sup>2</sup> (Karingithi, 2000)

(2012) was carried out at the Science Institute, University of Iceland, and the results are presented in the conventional delta notation in ‰ relative to the VSMOW standard (Vienna Standard Mean Ocean Water). The accuracy of the measurements for deuterium was 0.7 ‰, and for  $^{18}\text{O}$  was 0.05 ‰.

TABLE 4: Stable isotope composition of precipitation, spring waters, fumarole steam, borehole fluids and Lake Naivasha water

Sample identity	Location	Sample description	Oxygen ( $\delta^{18}\text{O}\text{‰}$ )	Hydrogen ( $\delta\text{D}\text{‰}$ )
<sup>1</sup> Spring 1	Hell's gate	Warm	3.25	23.4
<sup>1</sup> Spring 2	Hell's gate	Warm	2.07	12.5
<sup>1</sup> Spring 3	Hell's gate	Warm	3.56	15.7
<sup>1</sup> Spring 4	Hell's gate	Warm	2.77	14.9
<sup>1</sup> Spring 5	Hell's gate	Warm	4.55	22.9
<sup>1</sup> Spring 6	Hell's gate	Warm	4.86	14.9
<sup>1</sup> Spring 7A	Hell's gate	Warm	3.69	16.2
<sup>1</sup> Spring 7B	Hell's gate	Warm	4.86	15.6
<sup>1</sup> Spring 8	Hell's gate	Warm	3.69	28.4
<sup>1</sup> Spring 10	Hell's gate	Warm	4.05	20.3
<sup>1</sup> Spring 11	Hell's gate	Warm	3.82	20.7
<sup>1</sup> Spring 12	Hell's gate	Warm	3.69	20
<sup>1</sup> Spring 13	Hell's gate		3.69	31.2
<sup>1</sup> Fumerole 1	Hell's gate		-0.5	9.1
<sup>1</sup> X-2 fumerole	Olkaria		-2.91	-6.2
<sup>4</sup> Ndabibi borehole	North of L. Naiv.	cold	-2.9	-11.8
<sup>4</sup> Olsuswa borehole	North of L. Naiv.	cold	3.1	20
<sup>3</sup> Local sample		precipitation	-5.05	-32.75
<sup>3</sup> Kinangop		Precipitation	-4.8	-28
<sup>1</sup> Mau Escarpment		precipitation	-0.33	-1.4
<sup>2</sup> 28	Eastern Rift wall	28°C	-4.8	-28
<sup>2</sup> 39	Eastern Rift wall	29°C	-4.5	-20
<sup>2</sup> 82	Eastern Rift wall	20°C	-4.1	-24
<sup>2</sup> 93	Eastern Rift wall	23°C	-3.5	-17
<sup>2</sup> 95	Western Rift wall	24°C	-3.5	-16
<sup>2</sup> 96	Eastern Rift wall	23°C	-4.7	-24
<sup>2</sup> 101	Western Rift wall	25°C	-5.3	-35
<sup>2</sup> 122	Western Rift wall	35°C	-4.8	-27
<sup>2</sup> Lake Naivasha			6.6	36

<sup>1</sup> (Sveinbjörnsdóttir, 1988); <sup>2</sup> (Allen and Darling, 1992);

<sup>3</sup> (Ojiambo and Lyons, 1993); and <sup>4</sup> (Sekento, 2012)

### 3.3 Characterization of reservoir fluid composition

Several physical processes may alter the isotopic characteristics of thermal waters during their ascent to the surface. These processes include: cooling by conduction; mixing of two different thermal waters; mixing of thermal waters with non-thermal waters; subsurface boiling and steam separation; as well as non-equilibrium surface evaporation. The recalculation of aquifer isotope composition is essential if the isotope composition of the thermal waters are to be used to trace their source. Cooling by conduction has not been known to cause characteristic changes in isotope composition of fluids. Shallow thermal aquifers are commonly prone to mixing with cooler waters, mainly originating from local precipitation, and mixing with thermal waters of meteoric origin that may originate in precipitation at higher elevation. The isotope signatures and the chemistry of these two water types are considerably distinct. The oxygen isotope ratio and the chloride content of the thermal waters help to distinguish between these water

types. Most of the wells drilled in the Olkaria geothermal field discharge fluids at high pressure. Therefore, the influence of cold water on shallow thermal reservoirs is considerably reduced. Isotopic fractionation, due to subsurface boiling and steam separation, is common in high temperature geothermal well fluids, such as those in the Olkaria field where aquifer temperatures are  $>200^{\circ}\text{C}$ . The fluid in these wells flows under pressure greater than the saturated vapour pressure and, therefore, a mixture of steam and water is discharged at the wellhead. Certain dissolved constituents in the liquid phase partition into the vapour phase, mainly the gases due to their low aqueous solubility. Most of the solutes initially dissolve in the liquid concentrate in the liquid phase and rarely partition into the vapour phase. Isotopes are also significantly fractionated during boiling. The light isotope oxygen 16 will concentrate in the vapour phase, while the corresponding oxygen-18 isotope is enriched in the liquid phase. Because of this fractionation, boiling in thermal waters will affect isotope composition, depending on the water-steam ratio and the mode of steam separation, i.e. single stage or continuous steam separation (Truesdell and Hulston, 1980). Liquid phase samples analysed by Sveinbjörnsdóttir (1988) were collected at atmospheric pressure at the weir box and, therefore, show enrichment in the heavier isotopes of deuterium and oxygen-18 as a result of boiling. The steam condensate was collected at 6 bar-a from most of the wells in the East field and in two wells from the Northeast field, wells OW-701 and OW-703. To calculate the deep fluid deuterium and oxygen-18 ratios for the water collected at 1 bar-a pressure, it is necessary to compute the water steam ratio at the point of sampling so as to recalculate the aquifer composition. The relative amount of water evaporating during adiabatic cooling in a well can be determined if the aquifer temperature is known. The well is assumed to receive the water in the liquid phase at a depth where the stationary pressure in the well is higher than the saturated vapour pressure of the water. When the water flows up the well, its temperature remains constant until the stationary pressure becomes equal to the saturated vapour pressure. At that point, the water begins to cool through adiabatic boiling; consequently, a mixture of steam and water is present in the well. As a result, the temperature of the water is lowered and the steam-to-water ratio increases as the mixture moves further upwards. This is expressed by the steam fraction denoted  $X$  in Equation 7:

$$X = \frac{H^{dl} - H^l}{H^v - H^l} \quad (7)$$

where  $H^{dl}$  is the enthalpy of saturated liquid at the reservoir temperature;  
 $H^l$  is the enthalpy of saturated liquid at the temperature of sampling;  
 $H^v$  is the enthalpy of saturated vapor at the temperature of sampling.

From the steam fraction calculated and the isotope fraction of the isotopes in the steam and water phases, the deep liquid composition can be computed from the conservation of mass equation expressed by Equation 8:

$$\delta_{dl} = \delta_l(1 - X) + \delta_v(X) \quad (8)$$

where  $\delta_{dl}$  is the reservoir composition;  
 $\delta_l$  and  $\delta_v$  are the isotope ratios of the composition of the liquid and vapour, respectively.

The above methodology for evaluating the composition of the deep reservoir fluid was applied when samples of the two phases were collected. This was not the case for Karingithi's (2000) samples when only the water samples were available for measurements and interpretation. For this case, isotope fractionation factors were defined at specific temperatures by Bottinga and Craig (1968), taking into account the fractionation factors' dependence on temperature coming into play. Assuming that vaporization within geothermal reservoirs takes place at a phase equilibrium with the net removal of steam, changes in the isotope ratios maybe determined. The isotope composition of the deep reservoir fluid can be computed from water samples using Bottinga and Craig's (1968) Equation 9, where the effective isotope fractionation factor for the separation of the isotopes between the two phases is considered to be the ratio of the components in the water and vapour phases, respectively, and assuming that equilibrium conditions were met during isotope fractionation. Then the effective isotope fractionation factors can be replaced by the equilibrium constant:

$$1000 \ln \alpha = A + B(10^3/T) + C(10^6/T^6) + D(10^9/T^3) \quad (9)$$

where  $\alpha_D = P_{H_2O}/P_{HDO}$  and  $\alpha^{18}O = P_{H_2^{16}O}/P_{H_2^{18}O}$  and the numerical values for the constants are:

	HDO-H <sub>2</sub> O	H <sub>2</sub> <sup>18</sup> O-H <sub>2</sub> <sup>16</sup> O
A	559.69	-7.174
B	-808.06	4.716
C	772.81	-0.058
D	-54.41	_____

From the formula of Bottinga and Craig (1968), it is found that the isotope fractionation factors at a temperature of 159°C, corresponding to a pressure of 6 bar-a, are given as  $1000 \ln \alpha_D = 11.9$  and  $1000 \ln \alpha^{18}O = 3.63$ . Therefore, assuming a single stage steam separation, the vapour phase concentration can be computed using Equation 10:

$$1000 \ln \alpha_{A-B} = \delta_A - \delta_B \quad (10)$$

where  $\delta_A$  and  $\delta_B$  denote the respective ratios in the two phases.

Reservoir oxygen and deuterium isotope fluid composition for the Karingithi (2000) data was then computed using Equations 11 and 12, respectively:

$$(\delta D)_{dl} = (\delta D)_1 - X_{6\text{bar a}} \times 1000 \ln \alpha(D) \quad (11)$$

$$(\delta^{18}O)_{dl} = (\delta^{18}O)_1 - X_{6\text{bar a}} \times 1000 \ln \alpha(^{18}O) \quad (12)$$

### 3.3.1 Comparison between the two methods of reservoir fluid characterization

Table 5 shows the isotope ratio for reservoir fluid calculated using mass balance equations and isotope fractionation constants at the sampling temperatures. The  $\Delta$  isotope ratio shows the difference between the two methods for evaluating the deep reservoir fluid, one using the conservation of mass equation where the two phases are available, and the other using isotope fractionation factors where only the liquid phase is available. From the computations, the calculated reservoir fluid oxygen-18 values agree quite well. The difference for the deuterium values of the deep reservoir fluid varies between  $\delta D = -3.60\text{‰}$  and  $\delta D = 0.23\text{‰}$ . For some wells, the difference is much greater between the calculated deuterium isotope composition of the steam phase and the measured composition, but this difference is not seen in the computation of the reservoir fluid because the calculated steam fraction is relatively low.

## 4. RESULTS AND DISCUSSION

### 4.1 The $\delta D - \delta^{18}O$ relationships

#### *Springs and boreholes*

Figure 4 shows the water isotope composition of springs and boreholes within the Olkaria geothermal field. This is plotted along with a sample from Lake Naivasha and precipitation from the Naivasha area (local) and Kinangop. This is then plotted along with the Continental Africa rain line (CARL) and the Kenya Rift Valley evaporation line (KRVEL), defined by Ármannsson (1994) and Clarke et al. (1990), respectively. The Lake Naivasha sample shows enrichment in the isotope ratios with  $\delta D = 36\text{‰}$  and  $\delta^{18}O = 6.6\text{‰}$ . This enrichment in the stable isotope ratios is explained by evaporation to which the lake water is subject. The precipitation samples show a depletion in the stable isotope ratios, i.e.  $\delta D = -28\text{‰}$ , and  $\delta^{18}O = -4.8\text{‰}$  for the Kinangop sample, and slightly lower  $\delta D = -32.7\text{‰}$  and  $\delta^{18}O = -5.05\text{‰}$  for the local precipitation. The isotope composition of groundwater is represented by 13 warm springs sampled

TABLE 5: Aquifer composition calculated

Well	Location	H <sub>0</sub> (kJ/kg)	WB		Steam Oxygen (δ <sup>18</sup> O‰)	Steam Hydrogen (δD‰)	Calculated steam phase		Steam fraction(X) at 6 bar a	#Reservoir fluid Oxygen (δ <sup>18</sup> O‰)	#Reservoir fluid Hydrogen (δD‰)	#Reservoir Calculated Oxygen (δ <sup>18</sup> O‰)	#Reservoir Calculated Hydrogen (δD‰)	ΔOxygen (δ <sup>18</sup> O‰)	ΔHydrogen (δD‰)	
			Oxygen (δ <sup>18</sup> O‰)	Hydrogen (δD‰)			Oxygen (δ <sup>18</sup> O‰) – 6 bara	Hydrogen (δD‰) – 6 bara								
'2	East	2287	3.78	18	-0.45	1.3	-0.69	2.09	0.22	2.18	11.16	2.13	11.34	0.05	-0.18	
'4		2350	5.35	32.6	-1.37	-4.2	0.68	14.38	0.19	3.21	20.38	3.61	23.98	-0.4	-3.6	
'6		2378	4.02	17.4	-0.78	-1.5	-0.28	2.62	0.17	2.67	11.87	2.75	12.55	-0.08	-0.68	
'10		2457	5.04	27.8	-0.39	1.1	0.67	11.83	0.15	3.62	20.42	3.77	21.99	-0.16	-1.57	
'11		2222	3.78	18.2	-0.39	2.3	-0.54	2.95	0.18	2.45	12.55	2.42	12.67	0.03	-0.12	
'13		2400	4.47	25.3	-0.11	7.5	-0.29	7.01	0.25	2.47	16.03	2.42	15.91	0.05	0.12	
'14		2600	4.75	25	0.54	9.4	0.2	8.24	0.19	3.19	18.05	3.12	17.82	0.07	0.23	
'15		2600	5.51	23.6	0.27	2.6	1.14	8.53	0.13	4.17	18.04	4.28	18.84	-0.12	-0.8	
'16		2150	4.16	17.6	-0.25	-0.8	-0.35	1.99	0.21	2.54	10.79	2.52	11.38	0.02	-0.59	
'17		2600	6.36	32	0.2	4.7	1.34	13.11	0.22	3.93	20.58	4.18	22.41	-0.25	-1.84	
'18		2596	5.46	25.5	0.44	5.6	0.9	9.25	0.17	3.83	18.5	3.91	19.12	-0.08	-0.62	
'19		2500	5.86	29	-0.18	-0.4	1.01	11.04	0.21	3.63	18.07	3.88	20.46	-0.25	-2.39	
'20		2300	4.36	20.2	-0.5	-0.3	-0.17	4.15	0.21	2.65	12.7	2.72	13.61	-0.07	-0.91	
'21		2390	6.29	36.3	-0.36	5.1	1.43	17.28	0.2	4	24.46	4.35	26.85	-0.35	-2.39	
'22		2610	4.85	26.7	-0.76	2.4	0.5	10.84	0.15	3.41	19.72	3.59	20.98	-0.19	-1.25	
'23		2400	5.7	26	0.49	6.6	0.95	9	0.2	3.78	18.1	3.87	18.57	-0.09	-0.47	
'24		2460	4.19	20.3	-0.3	3.2	-0.36	3.92	0.22	2.48	13.04	2.47	13.2	0.01	-0.16	
'25		1920	3.76	17.8	-0.6	-0.5	-0.69	2	0.22	2.16	10.75	2.14	11.3	0.02	-0.55	
'26		2025	4.38	24.2	-0.16	6.8	-0.05	7.87	0.18	2.89	17.39	2.91	17.59	-0.02	-0.2	
'701		North East	1255	3.45	24	-1.06	3.9	-0.82	7.66	0.19	2.1	16.66	2.14	17.36	-0.04	-0.7
'703			1820	4.3	32.9	-1.03	3.7	-0.03	15.62	0.16	2.91	24.05	3	25.57	-0.16	-1.95
'2709			1047	4.18	23.7			-0.32	6.9	0.21			2.56	16.33		
'2714			1125	3.71	23.7			-0.65	7.11	0.2			2.26	16.66		
'2719			1037	3.43	22.3			-0.93	5.67	0.21			1.93	15.05		
'301		West	1180	-0.16	-1.7			-3.75	-13.18	0.24			-1.01	-4.19		
'302			1130	0.87	7.6			-2.95	-5.97	0.22			-0.12	3.31		
'304		874	-2.21	-9.3			-5.62	-20.29	0.1			-2.35	-9.55			
'306		1018	-0.04	0.5			-3.66	-11.48	0.17			-0.64	-1.57			
'307		852	-2.02	-5.8			-5.47	-17.19	0.09			-2.16	-6.33			
'308		780	-4.55	2.5			-7.94	-9.53	0.05			-4.5	1.74			
'901	Domes	1600	4.97	32.2			0.38	14.05	0.19			3.3	23.64			
'902		1338	3.22	21.8			-1.18	4.71	0.24			1.59	13.77			
'903		1073	3.09	21.7			-1.12	5.75	0.19			1.83	15.42			
'914A		2236	-	-			-	-				-0.54	8.2			
'916A		2500	-	-			-	-				3.63	21.02			

<sup>1</sup> (Sveinbjörnsdóttir, 1988); <sup>2</sup> (Karingthi, 2000); <sup>3</sup> (measurements by ISOR in 2010); # - calculated using mass balance equation

around the Hell's gate area, and two cold boreholes, Olsuswa and Ndabibi, located north of Lake Naivasha. The  $\delta D - \delta^{18}O$  relationship shows that the spring data cluster close to the KRVEL, gives a mean of  $\delta^{18}O = 3.7\text{‰}$ , and a standard deviation of  $0.9\text{‰}$ . The mean  $\delta D = 17.9\text{‰}$  with a standard deviation of  $3.7\text{‰}$ , excluding springs 8 and 13 which indicate a relatively high deuterium content of  $\delta D = 28.4\text{‰}$  and  $\delta D = 31.2\text{‰}$ , respectively. The evapo-concentrated groundwater on the Rift floor has been suggested to be flowing in both northerly and southerly directions. Therefore, enrichment in the isotope ratios of the spring samples collected south of the lake indicates that their recharge is partly from an evaporated source. The Olsuswa and Ndabibi boreholes are located close to each other, but the water from these two boreholes shows different isotope ratios. The Ndabibi borehole water is depleted in oxygen-18 to about  $\delta^{18}O = -2.9\text{‰}$  and deuterium to about  $\delta D = -11.8\text{‰}$ , while water from the Olsuswa borehole is enriched in oxygen-18 to about  $\delta^{18}O = 3.1\text{‰}$  and deuterium to about  $\delta D = 20\text{‰}$ . This difference in the isotope ratio indicates that the Ndabibi borehole is getting its recharge mainly from precipitation, whereas the Olsuswa borehole is mainly recharged from the evapo-concentrated source. The difference in the isotope ratios between these two very close boreholes could, therefore, be explained with reference to underground channels that control fluid movements in the area. The deuterium ratio in all these samples, except that from the Olsuswa borehole, is significantly higher than the deuterium ratio of the local precipitation. Therefore, it is suggested that precipitation around the Naivasha area contributes insignificantly to groundwater in the area. However, more isotope data on precipitation in the area is needed to conclusively confirm this.

*Samples from wells*

Figure 5 shows the relationship between the vapour phase and the liquid phase isotope ratios of samples of thermal origin. The figure demonstrates that liquid samples are enriched in both oxygen-18 and deuterium, relative to their corresponding vapour phase samples. The isotope composition of fluids from Fumarole 1 and Fumarole X-2, located in the Hells Gate

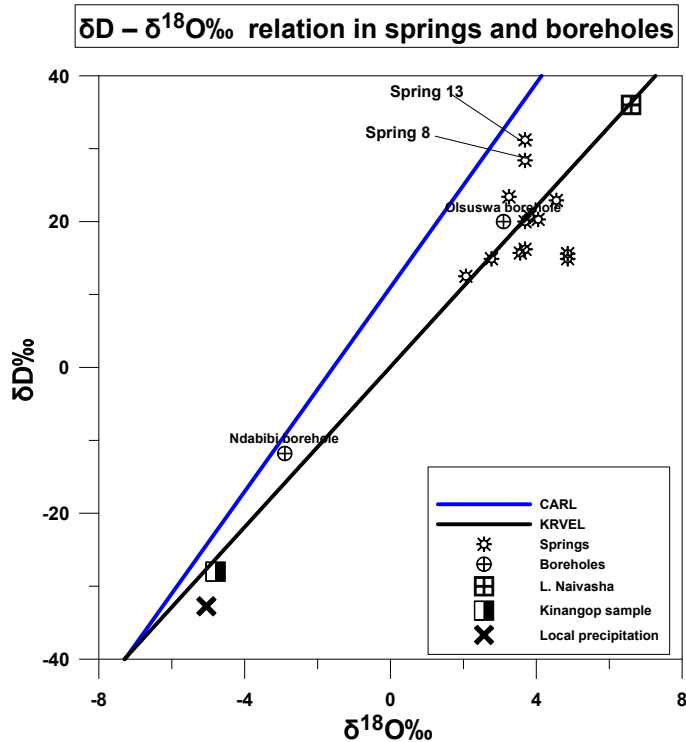


FIGURE 4: The  $\delta D - \delta^{18}O$  relationships of springs and borehole water in the area around Olkaria geothermal field

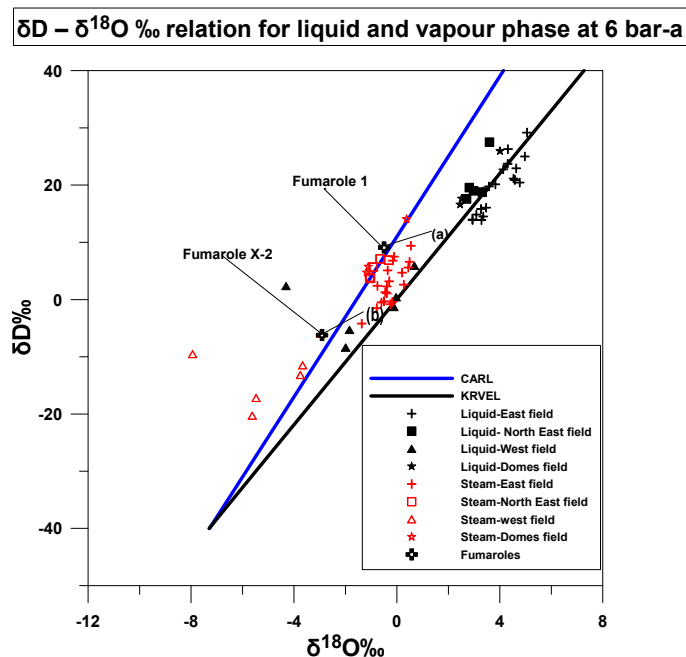


FIGURE 5: The  $\delta D - \delta^{18}O$  relationship between liquid and vapour phase isotope ratios at 6 bar-a of Olkaria geothermal wells

area, are also shown in Figure 5. Fumarole 1 fluid shows depletion in the oxygen-18 ratio to about  $\delta^{18}\text{O} = -0.5\text{‰}$ , and enrichment in the deuterium isotope ratio to about  $\delta\text{D} = 9.1\text{‰}$ , whereas Fumarole X-2 fluid shows depletion in both the oxygen-18 and deuterium ratios to about  $\delta^{18}\text{O} = -2.91\text{‰}$  and  $\delta\text{D} = -6.2\text{‰}$ , respectively. Assuming single stage steam separation, and that the samples from the two fumaroles tap fluids at reservoir temperatures close to the well temperatures in the area, then the liquid composition can be defined as shown in the plot as (a) and (b). From the figure, it can be seen that the isotope composition of Fumarole X-2 (b) is very close to that of the wells in the Olkaria West field, whereas Fumarole 1 (a) fluid is more related to that of the East field, although less influenced by the evapo-concentrated water source.

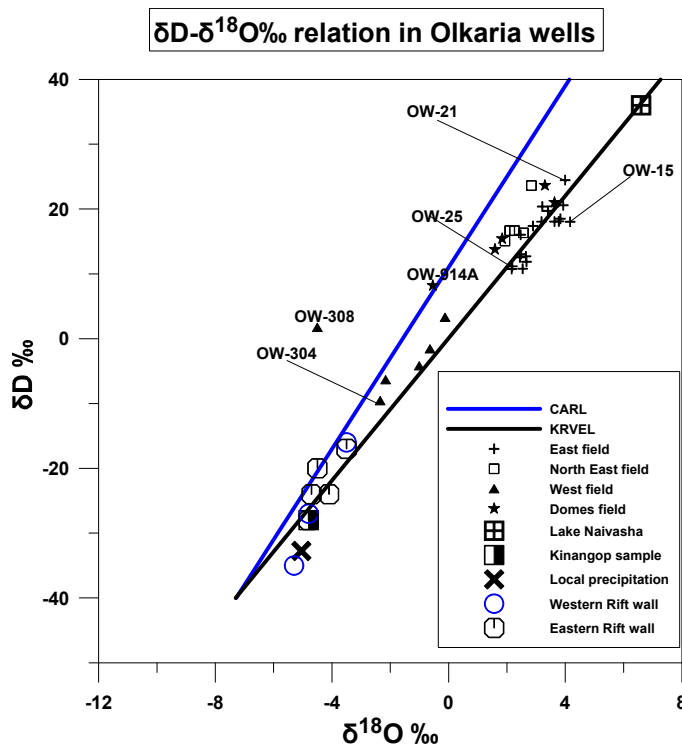


FIGURE 6: The  $\delta\text{D}-\delta^{18}\text{O}$  relationship of aquifer fluids in Olkaria wells

than that from well OW-25, which shows the smallest oxygen shift ( $\delta^{18}\text{O} = 2.16\text{‰}$ ) in the field. The larger oxygen isotope shift observed in the aquifer fluids of well OW-15 could be interpreted as deep circulation, and extensive water-rock interaction associated with the water. The mean  $\delta\text{D}$  value for the 19 well samples is  $16.75\text{‰}$ , with a standard deviation of  $5.72\text{‰}$ , with enrichment of deuterium observed in well OW-21:  $\delta\text{D} = 24.46\text{‰}$ . This enrichment in the deuterium isotope ratio in the well OW-21 sample could be explained with a larger component of the evapo-concentrated source. In Figure 6, the Northeast samples also plot close to the evaporation line. The mean  $\delta^{18}\text{O} = 2.35\text{‰}$  is slightly lower than that from the East field. This could be a result of a high water-rock ratio, which could obscure oxygen isotope shifts in the fluids. The highest reported deuterium isotope ratio for the Northeast field samples is  $\delta\text{D} = 24.05\text{‰}$ , which is close to what was reported for the East field samples. Therefore, despite these two fields being located at some distance from each other, they still seem to get most of their recharge from the evapo-concentrated source, thus implying that these two subfields are hydro-geologically connected, and there possibly exist underground flow channels connecting these two fields to the same recharge. The Domes field samples, similar to the East field and the North East samples, plot close to the evaporation line, with the exception of the sample from well OW-914A which plots on the precipitation line. The well OW-914A sample exhibits isotope ratios of  $\delta^{18}\text{O} = -0.54\text{‰}$   $\delta\text{D} = 8.20\text{‰}$ ; the well OW-916A sample, exhibiting  $\delta^{18}\text{O} = 3.63\text{‰}$  and  $\delta\text{D} = 21.02\text{‰}$  is located in the southeast part of the Domes field, Figure 7, shows distinct isotopic signatures despite the fact that these two wells are 800 m apart.

The  $\delta\text{D} - \delta^{18}\text{O}$  relationship of the estimated aquifer fluid isotope composition within the Olkaria geothermal field is shown in Figure 6, along with that of groundwater from the eastern and western Rift walls, local and Kinangop precipitation, as well as Lake Naivasha water. In the figure, it can be seen that most of the groundwater from the Rift wall plots close to the intersection between the precipitation and the evaporation lines with isotope ratios of about  $\delta^{18}\text{O} = -4.8\text{‰}$  and  $\delta\text{D} = -28\text{‰}$ , respectively, which is characteristic of high altitude precipitation. The Olkaria East field wells are mainly located on NW-SE and NE-SW trending faults, shown in Figures 7a and 7b. Isotope results are available for 19 wells in the East field, illustrated in Figure 6. These samples tend to cluster along the evaporation line. The mean oxygen-18 ratio is  $\delta^{18}\text{O} = 3.12\text{‰}$  with a standard deviation of  $0.66\text{‰}$ . This shows that these samples have a relatively similar oxygen isotope ratio. The sample from well OW-15, located in the East field, shows a larger oxygen isotope shift ( $\delta^{18}\text{O} = 4.17\text{‰}$ )



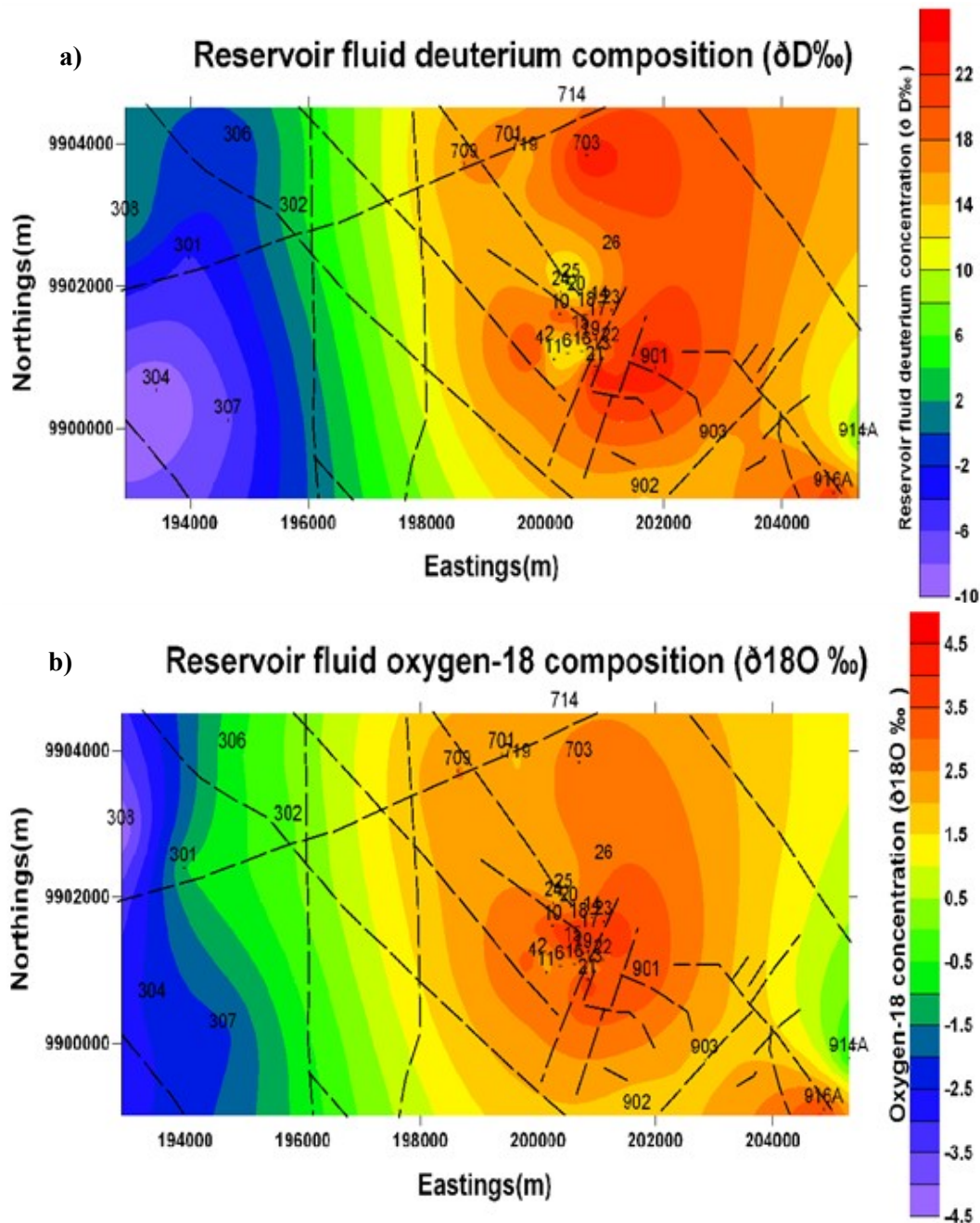


FIGURE 7: Shows the distribution of a) aquifer deuterium, and b) oxygen-18 isotope ratios associated with the structural geology of the Olkaria geothermal field

This could be explained by the effects of faults that control fluid movement in the area. The NW-SE trending fault cutting through well OW-916A, as shown in Figure 7, could possibly be acting as a barrier to escarpment water from the eastern flank which is possibly recharging well OW-914A. The possibility of the ring structure also controlling fluid movement cannot be ruled out, but that cannot be confirmed because of the scarcity of data from the area. The Olkaria West field exhibits a distinctly different recharge source compared to the rest of the fields. The samples from this field show a mean of  $\delta^{18}O = -1.80\text{‰}$  and  $\delta D = -2.77\text{‰}$  with well OW-304 fluid having a deuterium isotope ratio of  $\delta D = -9.55\text{‰}$ . It is suggested that these wells get their recharge from groundwater from the western Rift wall. The samples also indicate that there could be some mixing between water from an evapo-concentrated source and the rift wall groundwater along the evaporation line, with the waters of the rift wall providing a major contribution to the aquifers in this field. The negative oxygen isotope shift seen in the aquifer fluid of well OW-308 of the West field could be a result of  $CO_2$  bubbling, caused by bicarbonate type

waters discharged in this field. The depleted deuterium content indicates lighter fluids, characteristic of fluids from high altitudes.

**4.2 Evolution of reservoir fluid isotope composition of wells in Olkaria geothermal field**

Table 6 shows the isotope composition variation with time for 6 wells in the Olkaria geothermal field. Data was obtained by Allen and Darling (1987), Sveinbjörnsdóttir (1988), and Karingithi (2000).

TABLE 6: Variations of reservoir Isotope ratios with time

Wells	1987		1988		2000	
	Oxygen ( $\delta^{18}O\text{‰}$ )	Hydrogen ( $\delta D\text{‰}$ )	Oxygen ( $\delta^{18}O\text{‰}$ )	Hydrogen ( $\delta D\text{‰}$ )	Oxygen ( $\delta^{18}O\text{‰}$ )	Hydrogen ( $\delta D\text{‰}$ )
OW-10	-1.71	-7.92	3.73	20.88	3.24	15.68
OW-16	2.48	4.42	2.54	9.02	2.18	6.52
OW-23	2.65	5.80	4.15	18.70	3.04	13.50
OW-15			4.26	16.99	3.12	13.09
OW-19			2.15	9.27	2.49	10.47
OW-25			4.20	20.21	3.37	18.61

Figure 8 shows characteristic changes of reservoir fluid deuterium composition in 6 wells in the East field, sampled between 1987 and 2000. Wells OW-15, OW- 19 and OW-25 have available results only for the years 1988 and 2000, whereas results for wells OW-10, OW-16 and OW-23 are available for the years 1987, 1988 and 2000. The isotopic results show a drastic increase in the water isotope composition between the years 1987 and 1988. The much depleted value for well OW-10, compared to the other wells sampled at the same time, could be an analytical error. The figure also shows a decrease in the isotope ratio between the years 1988 and 2000 for almost all wells. This could be explained by temporal variations associated with recharge waters, particularly the amount of rainfall and the average relative humidity which affect the degree of evaporation in the area.

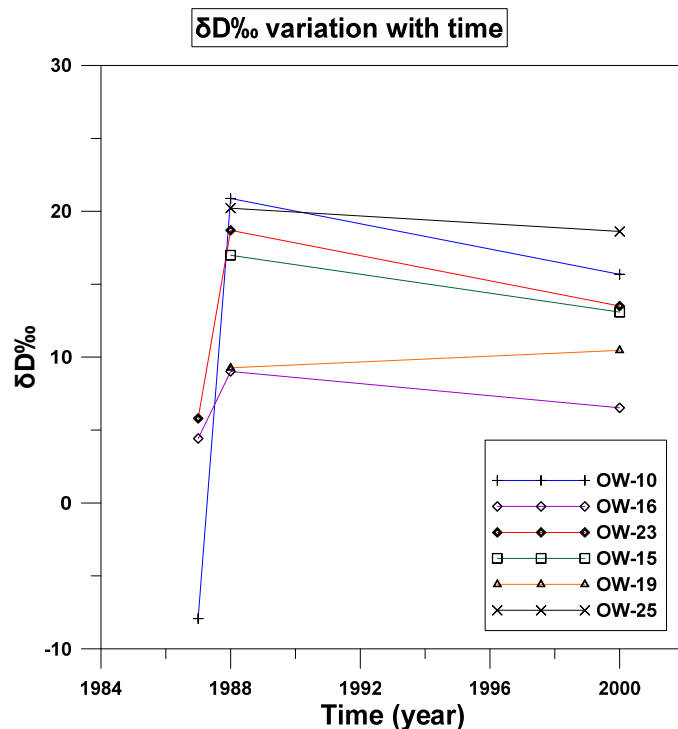


FIGURE 8: A plot showing deuterium isotope ratio variation with time in 6 wells sampled between years 1987 and 2000

**4.3 Mixing of evapo-concentrated water with escarpment recharge water**

A  $\delta D$ -Cl plot is presented in Figure 9. The figure shows that groundwater from the Rift wall and the evapo-concentrated water have a similar chloride concentration. This limits the use of chloride in indicating mixing patterns between these two recharge waters. It can be seen from the plot that the evapo-concentrated water contributes more to the recharge of most of the aquifer fluids than groundwater from the rift walls. The east, northeast and southeast parts of the Domes field show relatively similar deuterium isotope ratios, but the aquifer Cl concentrations of fluids in these fields

varies considerably between 300 mg/kg and about 1000 mg/kg in the East field, indicated in Figure 10, where the regional distribution of chloride is demonstrated. The Northeast field samples seem to lie between the two extreme cases. This high chloride could be explained as uptake of the chloride from the rocks or could possibly indicate upflow of deep geothermal fluid (Karingithi, 2000) which could be related to deep circulation of the recharge water in these fields. The West field fluid chloride concentration is relatively low or about 200 mg/kg.

**4.4 The stable deuterium isotope as a natural tracer**

The hydrogen isotope is the most widely used conservative isotope because it is inert and highly mobile (Arnórrsson, 2000). It has been used extensively as a tracer to locate recharge zones to geothermal reservoirs because the water content of all common rocks is considered so low that isotopic exchange involving the hydrogen isotope is insignificant.

Therefore, the deuterium content of the waters will effectively not change during underground passage of water. However, its application as a natural tracer depends on the following assumptions: the groundwater is meteoric in origin; no changes in the isotope ratio take place underground; climatic conditions have not changed significantly in the area for at least 8000 years (Árnason, 1976). Reservoir fluid

deuterium has been used to trace the flow of recharge water in the Olkaria geothermal field, as indicated in Figure 11. The fluids recharging the East, Northeast and a part of the Domes field are waters showing enrichment in the hydrogen isotope; the waters recharging most of the aquifers in the West field and the southeast part of the Domes field indicate recharge from the escarpments.

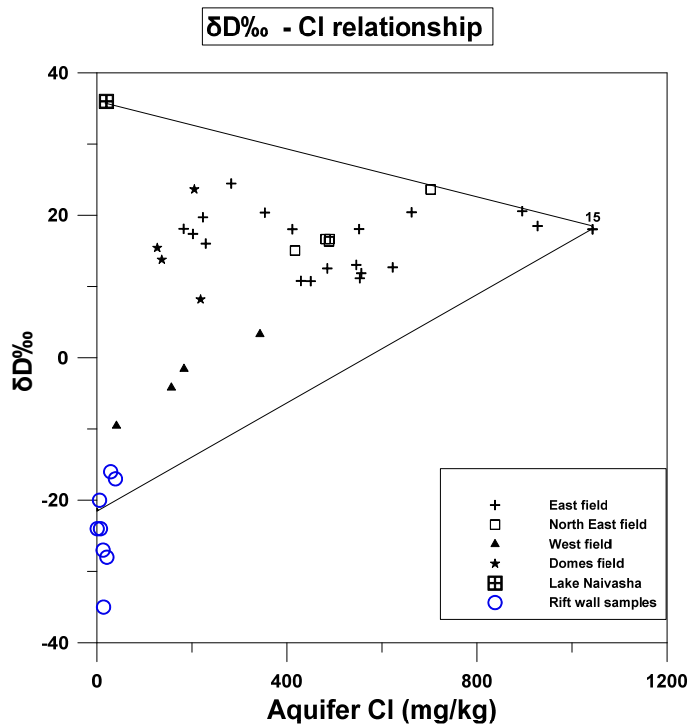


FIGURE 9: Aquifer δD-chloride relationship of wells in the area

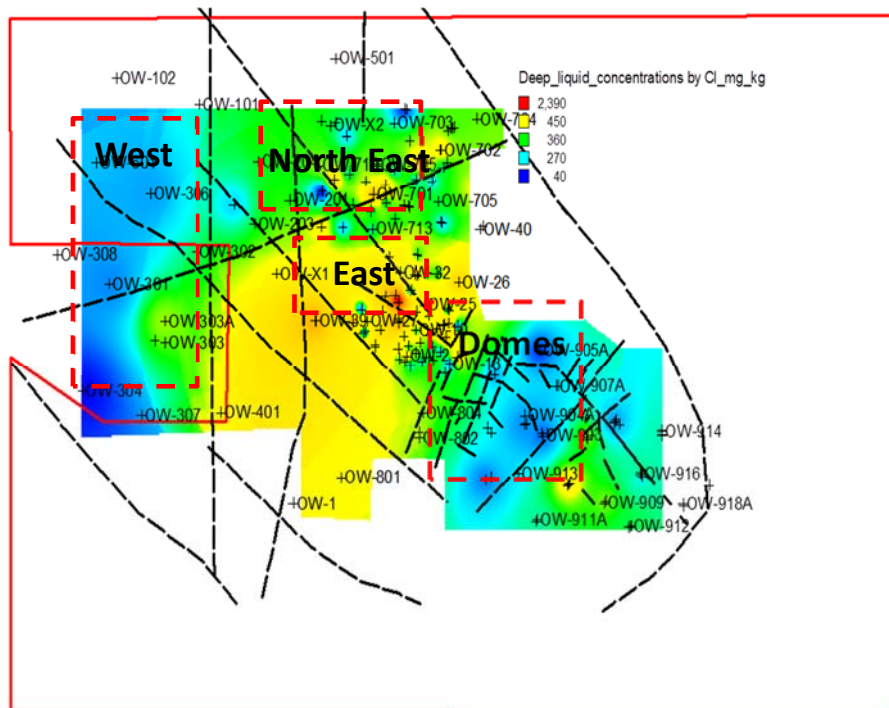


FIGURE 10: A contour map showing the Olkaria reservoir fluid chloride distribution map

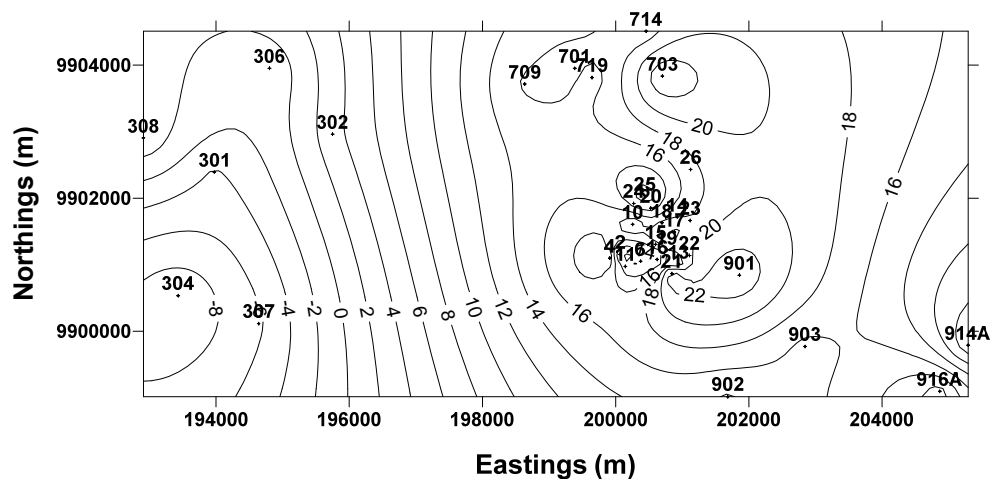


FIGURE 11: A contour map showing aquifer deuterium composition of wells in Olkaria field

#### 4.5 A conceptual hydrological model of the Olkaria geothermal field

The thermal waters discharged in the Olkaria geothermal field are meteoric in origin. They are derived from high altitude precipitation through fault systems acting as underground channels; they reach greater depths where they acquire chloride from magmatic gases input or some amounts from host rocks and heat from volcanic intrusions in the area and, finally, through faults and fissures on the Rift floor. The Olkaria water isotope compositions suggest mixing of at least three components. These include groundwater from the eastern Rift wall, groundwater from the western Rift wall, and characteristic evapo-concentrated water. The deep thermal inflow into the Olkaria East and North East fields is enriched in the hydrogen isotope ratio, compared to local precipitation, as well as to precipitation from a high elevation,  $\delta D = 24.46\text{‰}$ ; the oxygen isotope shift varies between  $\delta^{18}O = 2.35$  and  $\delta^{18}O = 3.12\text{‰}$ . The most depleted waters in the field are reported in the West field with  $\delta D = -9.55\text{‰}$  and an oxygen isotope shift of  $\delta^{18}O = -2.77\text{‰}$ . The fluids discharged in the Domes show a considerable range in the isotope ratio, suggesting mixing of the evapo-concentrated water with distant water to varying degrees.

The isotope composition of fumaroles and spring samples from the area indicates that the recharge is from Rift wall waters and evapo-concentrated water. The aquifer waters in Olkaria East, Northeast and some of the Domes wells get their recharge from the evapo-concentrated source, whereas the West field seems to be recharged by waters from the western Rift wall. Mixing of these water types is along the  $\delta D - \delta^{18}O$  evaporation line with the evapo-concentrated water contributing largely to the recharge waters of the East and Northeast fields. The Domes field seems to be recharged by groundwater from the eastern Rift wall mixing with evaporated water, as indicated by results for some wells in the area. The contribution of the evaporated water to the West field is minimal, as reflected in the hydrogen isotope ratio of the aquifer fluids.

## 5. CONCLUSIONS

- The deuterium content of thermal waters within the Olkaria system has proven to be very useful in tracing the origin of the thermal water. Scarcity of isotope data, however, limits detailed interpretation of the groundwater hydrology.
- The Olkaria high temperature field receives a characteristic recharge from the Rift wall, and groundwater from an evapo-concentrated source recharges most of the wells in the area. Possible mixing of these waters is variable and dependent mostly on the influence of a fault system on the hydrology of the area.

- Olkaria West and the southeast part of the Domes area are least affected by recharge from the evaporated recharge water.
- The use of isotope fractionation factors and mass balance equations to characterize reservoir fluid composition yield coherent results for the oxygen-18 isotope ratios, but the deuterium isotope ratios vary to some extent.
- For six wells, more than one sample was available; the evolution of the water isotope ratios for these geothermal wells shows some changes in the isotope ratio of the water with time. This could be explained by temporal variations related to variations in the isotope composition of the recharge fluids.
- More work on isotope studies is ongoing and samples from recently drilled wells from the field have been collected together with new samples from older wells. The isotope composition of the samples will be determined at the Science Institute, University of Iceland. The results will be used to monitor variations in the hydrological regime of the area.

### ACKNOWLEDGEMENTS

I would like to extend my appreciation to the Government of Kenya and Kenya electricity generating company - KenGen for granting me the opportunity to attend this training programme. I am also greatly indebted to Mr. Lúdvík S. Georgsson, director of the UNU Geothermal Training Programme, for his time and guidance during the six month period. Many thanks to Ms. Málfríður Ómarsdóttir, Mr. Markús A.G. Wilde, Mr. Ingimar G. Haraldsson and Ms. Thórhildur Ísberg for making the six months a great learning experience. Sincere gratitude goes to my supervisors, Halldór Ármannsson of ISOR and Dr. Árný Sveinbjörnsdóttir of the University of Iceland, for your time, patience and endless effort to make this work a success; your comments are highly appreciated. I would also wish extend my appreciation to the UNU-GTP 2014 fellows for sharing their knowledge and experience. Thanks to the chemistry group for the wonderful time and great company we have had together.

Special thanks to my family, my sister Josephine Milanoi, for your support, encouragement and prayers during my stay in Iceland. Finally, I am grateful to the Almighty God for guidance and blessings throughout the entire training period

### REFERENCES

- Allen, D.J., and Darling, W.G., 1987: *Kenya Rift Valley geothermal project: Hydrogeology progress report*. British Geological Survey, report WD/OS/87/16, 65 pp.
- Allen, D.J., and Darling, W.G., 1992: *Geothermics and hydrology of the Kenya Rift Valley between Lake Baringo and Lake Turkana*. British Geological Survey, report SD/92/1, 39 pp.
- Allen D.J., Darling, W.G., and Burgess, W.G., 1989: *Geothermics and hydrogeology of the southern part of the Kenya Rift Valley with emphasis on the Magadi-Nakuru area*. British Geological Survey, report SD/89/1, 68 pp.
- Ármannsson, H., 1994: *Geothermal studies on three geothermal areas in West and Southwest Uganda*. UNDES, UNDP project UGA/92/002, report, 85 pp.
- Árnason, B., 1976: *Groundwater systems in Iceland traced by deuterium*. Soc. Sci. Islandica 42: 1-236.
- Arnórsson, S., 2000: Reactive and conservative components. In: Arnórsson, S. (ed.), *Isotopic and chemical techniques in geothermal exploration, development and use. Sampling methods, data handling, interpretation*. International Atomic Energy Agency, Vienna, 40-48.

- Arusei, M.K., 1991: *Hydrochemistry of the Olkaria and Eburru geothermal fields, Kenyan Rift valley*. UNU-GTP, Iceland, report 2, 39 pp.
- Bottinga, Y., and Craig, H., 1968: High temperature liquid-vapour fractionation factors for  $\text{H}_2\text{O}/\text{H}_2\text{O}^{18}$ . *Trans. Am. Geophys. Union*, 49, 356-357.
- Clarke, M.C.G., Woodhall, D.G., Allen, D., and Darling G., 1990: *Geological, volcanological and hydrogeological controls on the occurrence of geothermal activity in the area surrounding Lake Naivasha, Kenya, with coloured 1:100 000 geological maps*. Ministry of Energy, Nairobi, 138 pp.
- Coleman, M.L., Shepard, T.J., Durham, J.J., Rouse, J.E., and Moore, G.R., 1982: Reduction of water with zinc for hydrogen isotope determination. *Anal. Chem.*, 54, 993-995.
- Epstein, S., and Mayeda, T., 1953: Variations of  $^{18}\text{O}$  content of waters from natural sources. *Geochim. Cosmochim. Acta*, 4, 213-224.
- Fournier, R.O., and Potter, R.W. II, 1982: A revised and expanded silica (quartz) geothermometer. *Geoth. Res. Council, Bull.*, 11-10, 3-12.
- Geyh, M., 2000: Volume IV: Groundwater – Saturated and unsaturated zone. In: Mook, W.G., (editor), *Environmental isotopes in the hydrological cycle – Principles and applications*. International Hydrological Programme, IHP-V, Technical Documents in Hydrology, IV (39), UNESCO, Paris.
- Giggenbach, W.F. and Stewart, M.K., 1982: Processes controlling the isotopic composition of water discharges from steam vents and steam-heated pools in geothermal areas. *Geothermics*, 11, 71-80.
- Horita, J., 1988: Hydrogen isotope analysis of natural waters using an  $\text{H}_2$ -water equilibrium method: A special implication to brines. *Chem. Geol. (Isotope Geosc. Sec.)*, 72, 89-94.
- Karingithi, C.W., 2000: *Geochemical characteristics of the Greater Olkaria geothermal field, Kenya*. Report 9 in: *Geothermal training in Iceland in 2000*. UNU-GTP, Iceland, 165-188.
- Lagat, J.K., 2004: *Geology, hydrothermal alteration and fluid inclusion studies of the Olkaria Domes geothermal field, Kenya*. University of Iceland, MSc thesis, UNU-GTP, Iceland, report 2, 79 pp.
- McCann, D.L., 1972: *Preliminary hydrogeological evaluation of the long-term yield of catchment related to the geothermal prospect areas in the Rift Valley of Kenya*. UN report, 23 pp.
- McCann, D.L., 1974: *Hydrogeologic investigation of the Rift valley catchments*. Unpublished UN report, 47 pp.
- Mwania, M., Kandie, R., and Ronoh, I., 2014: *An update of geological conceptual model of the Greater Olkaria geothermal field*. KenGen, Kenya, internal report.
- Ojiambo, B.S., and Lyons, W.B., 1993: Stable isotope composition of Olkaria geothermal fluids, Kenya. *Geothermal Res. Council, Trans.*, 17, 149-153.
- Panichi, C., and Tongiorgi, E., 1974: *Isotope study of the hot water and steam samples of the Rift Valley*. UNDP report.
- Sekento, L. R., 2012: *Geochemical and isotopic study of the Menengai geothermal field, Kenya*. Report 31 in: *Geothermal training in Iceland in 2012*. UNU-GTP, Iceland, 769-792.
- Sikes, H.L., 1935: Notes on hydrology of Lake Naivasha. *J. East Africa & Uganda Nat. Hist. Soc.*, 14.
- Sveinbjörnsdóttir, Á.E., 1988: *Results of stable isotope measurements on samples from the Olkaria and Eburru geothermal fields, Kenya*. Kenya Power Company, Ltd., Science Institute, University of Iceland, report.
- Truesdell, A.H., and Hulston, J.R., 1980: Isotopic evidence on environments of geothermal systems. In: Fritz, P., and Fontes, C., *A handbook of environmental, isotope geochemistry*. vol. 1, ch. 5, 179-226.
- Truesdell, A.H., Nathanson, M., and Rye, R.O., 1977: The effects of subsurface boiling and dilution on the isotopic compositions of Yellowstone thermal waters. *J. Geophys. Res.* 82-26, 3694-3704.